

3D NUMERICAL STUDY OF HYDRODYNAMICS AROUND A MONOPILE FOUNDATION UNDER COMBINED WAVE CURRENT EFFECT

Subhrangshu Purkayastha, Indian Institute of Technology Kharagpur, subhrangshu.purkayastha@iitkgp.ac.in

Debasish Dutta, Indian Institute of Technology Kharagpur, debasish.dutta@iitkgp.ac.in

Mohammad Saud Afzal, Indian Institute of Technology Kharagpur, saud@civil.iitkgp.ac.in

Hans Bihs, Norwegian University of Science and Technology, hans.bihs@ntnu.no

ABSTRACT

A numerical investigation of hydrodynamics around a monopile foundation is presented in the paper. An open-source CFD program REEF3D is used for the present study. The REEF3D model solves the Reynolds-averaged Navier-Stokes equation with k- ω turbulence closure to obtain the flow hydrodynamics. The code utilizes a staggered cartesian grid system. Also, Message Passing Interface (MPI) based parallelization is used for domain decomposition. In order to ensure the precision of the flow field, the model is first validated for four different combined wave-current scenarios, where the currents and waves are following each other. The results obtained from the validation studies exhibit good agreement with the already reported experimental results. Initially, a grid convergence study has been performed to ensure that the Numerical wave tank is independent of the mesh size. Finally, numerical experiments corresponding to four different combined wave-current cases for different wave steepness are simulated using the code.

INTRODUCTION

The combined wave-current interaction in the coastal zone has great importance to determine mass and sediment transport rates because the sediment is picked up by the waves and transported by the mean horizontal flow. The combined wave-current motion changes the flow characteristics, horizontal and vertical velocities, turbulent intensities, and shear stresses. The present study investigates hydrodynamic characteristics for different combined actions of waves and current conditions, where waves and currents are following each other around an offshore pier. For numerical modeling, a computational setup is used which is the similar experimental setup used by Umeyama 2005. The wave-current interaction has gained the interest of coastal and marine engineers since it has a significant impact on sediment movement and seabed stability. Generally, the wave-induced vertical currents are responsible for the suspension of sediment particles (van Rijn 1993). Wave-current interaction can modify water pressure and shear stress at the seabed, affecting effective stress, pore water pressure, and displacement of soil, near the seafloor (Zhang et al. 2013). Flow around a group of circular cylinders in various configurations is significant in many engineering applications, and it has been the main focus of research in recent times. Out of those, two-cylinder arrangements have shown to be more effective in a variety of applications, including flow-through heat exchanger tubes, transmission cables, and offshore platforms (Wang et al. 2020). In

addition, behavior of flow around two cylinders offers a comprehensive view of the complicated behavior of various arrangements. In terms of cross-flow, the arrangement of two circular cylinders can be in tandem, staggered and side-by-side configurations. The development of shed vortices, separation of the shear layer, and propagation of wakes behind these cylinders arise complexity in the flow, especially in the side-by-side arrangement.

NUMERICAL MODEL

The open-source CFD model REEF3D [Bihs et al. (2016)] is chosen for the numerical demonstration of hydrodynamics around a monopile in a combined wave-current environment. The model has been effectively utilized for wave-current-structure interaction issues around the vertical piles and local scour issues. The numerical domain is discretized uniformly and Reynolds averaged Navier Stokes (RANS) equations are utilized to calculate the flow field. The continuity and momentum equation is shown as,

$$\frac{\partial U_i}{\partial x_i} = 0 \quad (1)$$

$$\frac{\partial U_i}{\partial t} + U_j \frac{\partial U_i}{\partial x_j} = \left[\frac{-1}{\rho} \frac{\partial P}{\partial x_i} + \frac{\partial (v + v_t)}{\partial x_i} \left(\frac{\partial U_i}{\partial x_j} + \frac{\partial U_j}{\partial x_i} \right) \right] + g_i \quad (2)$$

where u is the velocity averaged over time t , ρ is the fluid density, p is the pressure, ν is the kinematic viscosity, ν_t is the eddy viscosity and g is the acceleration due to gravity.

The convective elements of the RANS equations are discretized in a conservative finite difference framework employing the fifth-order weighted essentially non-oscillatory (WENO) method (Jiang and Shu 1996). The convective terms for the velocities u_j are solved using the conservative WENO scheme, whereas the components of turbulence and free surface are treated using the Jacobi-Hamilton version. For temporal discretization, a third-order total variation diminishing (TVD) Runge-Kutta approach is utilised (Gottlieb and Shu 1998). This technique possesses a high degree of temporal precision and exceptionally great numerical stability for Courant-Friedrichs-Lewy (CFL) values less than one. Further, adaptive time stepping is used to control the CFL number. All transport equations except turbulence model in the numerical wave tank are solved by applying the third-order TVD Runge-Kutta method in the numerical wave tank.

RESULTS

The numerical results of hydrodynamics around a pair of cylinders are compared with Umeyama (2005) experimental results in order to verify the REEF3D model results. Umeyama (2005) conducted the experiments using a tank of length 25 m, width of 0.7 m, and depth of 1 m. The current velocity and flow depth was 12 m/s and 20 cm respectively. The numerical results are validated with four different wave-current conditions as, (a) wave height (H) = 2.02 cm, wave period (T) = 0.9 s, (b) wave height (H) = 2.51 cm and wave period (T) = 1 s, (c) wave height (H) = 2.67 m and wave period (T) = 1.2 s, (d) wave height (H) = 2.8 m and wave period (T) = 1.4 s.

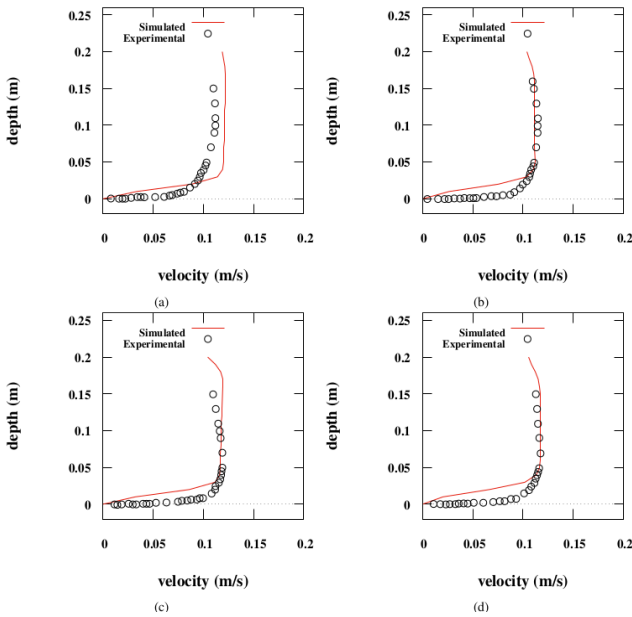


Figure 1 - Validation results of combined wave current hydrodynamics for different wave-current conditions

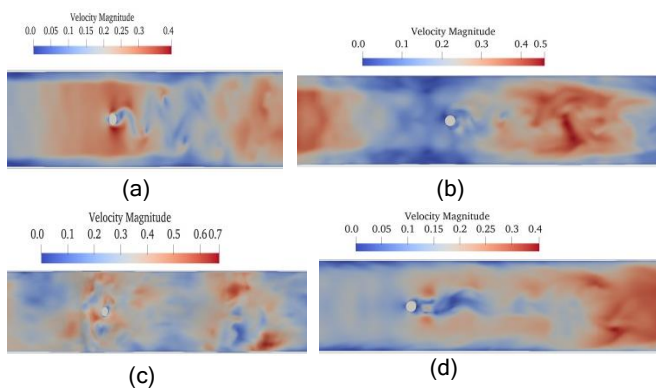


Figure 2 - Velocity Contour plot for different wave-current conditions (a) $U_{cw} = 0.87$, (b) $U_{cw} = 0.16$, (c) $U_{cw} = 0.44$, (d) $U_{cw} = 0.86$

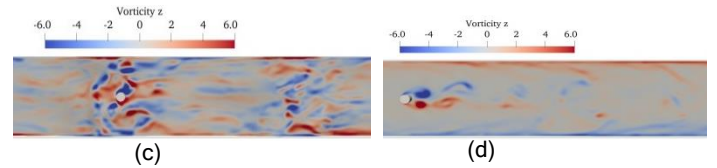
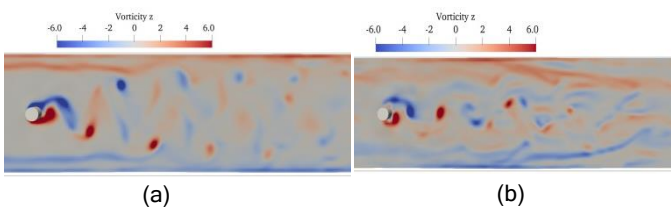


Figure 3 - Vorticity Contour plot for different wave-current conditions (a) $U_{cw} = 0.87$, (b) $U_{cw} = 0.16$, (c) $U_{cw} = 0.44$, (d) $U_{cw} = 0.86$

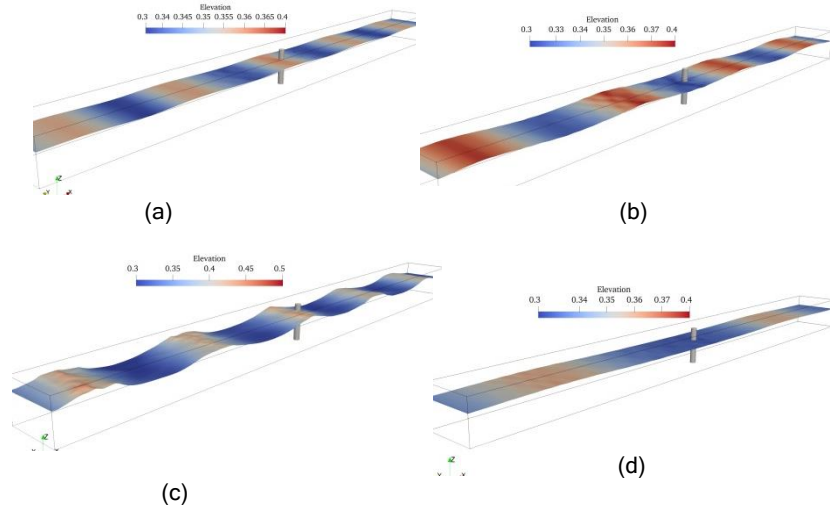


Figure 4 - Free surface elevations for different wave-current conditions (a) $U_{cw} = 0.87$, (b) $U_{cw} = 0.16$, (c) $U_{cw} = 0.44$, (d) $U_{cw} = 0.86$

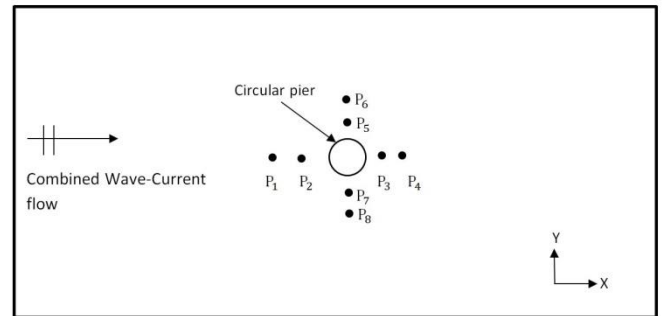
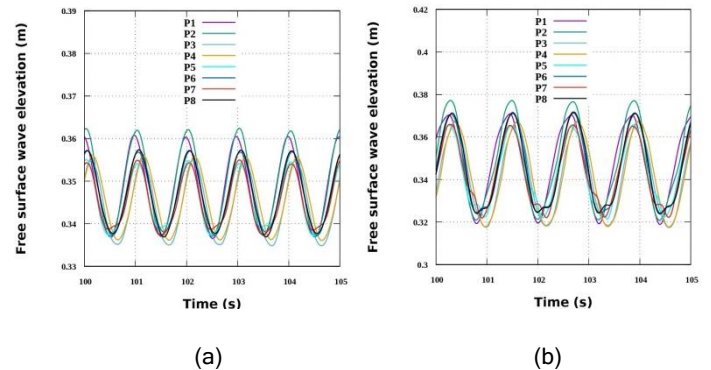


Figure 5 - Cross-section of computational domain for combined wave-current hydrodynamics around circular pile



(a)

(b)

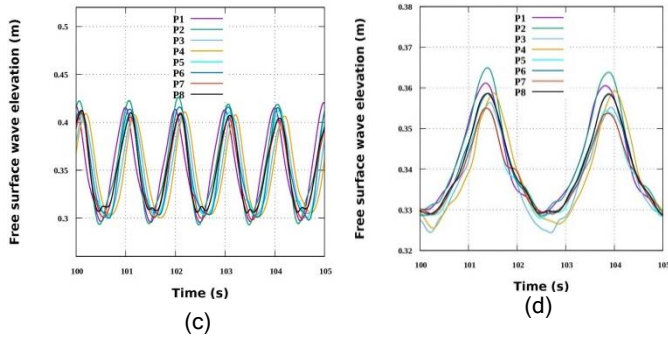


Figure 6 - Free surface elevation for different wave-current conditions (a) $U_{cw} = 0.87$, (b) $U_{cw} = 0.16$, (c) $U_{cw} = 0.44$, (d) $U_{cw} = 0.86$

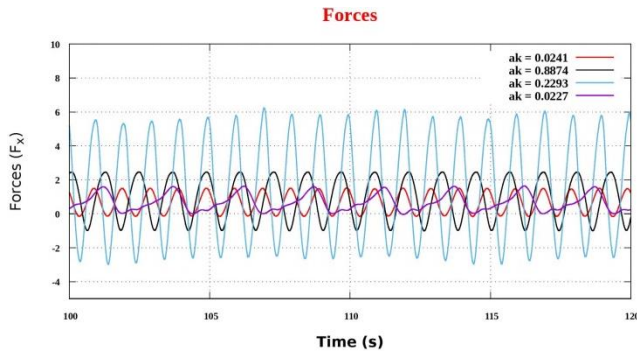


Figure 7 - Combined inline wave-current forces for different wave-current conditions (a) $U_{cw} = 0.87$ ($ak = 0.024$), (b) $U_{cw} = 0.16$ ($ak = 0.887$), (c) $U_{cw} = 0.44$ ($ak = 0.229$), (d) $U_{cw} = 0.86$ ($ak = 0.22$)

H	T	KC	U_w	U_c	U_{cw}	L	ak
0.018	1.5	0.16875	0.037	0.25	0.868	2.34	0.024
0.05	1.2	3.75	0.157	0.25	0.160	1.77	0.0887
0.1	1	0.625	0.31	0.25	0.443	1.37	0.229
0.03	2.5	0.46875	0.037	0.25	0.868	4.15	0.022

Table 1 - Tabular representation of combined wave-current parameters

CONCLUSION

Fig. 2 represents the velocity contour around the circular pile plot for different wave-current conditions (a) $U_{cw} = 0.87$, (b) $U_{cw} = 0.16$, (c) $U_{cw} = 0.44$, (d) $U_{cw} = 0.86$. Here the wave-current condition (a) and (d) presents the current dominated flow and (b) and (c) presents the wave dominated flow. The combined wave-current parameter (U_{cw}) is defined as given in Eq. 3.

$$U_{cw} = \frac{U_c}{U_c + U_m} \quad (3)$$

Fig. 3 represents the vorticity contours around the circular pile plot for different wave-current conditions (a) $U_{cw} = 0.87$, (b) $U_{cw} = 0.16$, (c) $U_{cw} = 0.44$, (d) $U_{cw} = 0.86$ at the end of the simulation period. For current dominated condition the shedding of vortices is clearly seen from Fig. 3. When the flow is wave dominated the mixing of vortices is seen from the

figures. Fig. 4 represents the free surface elevations for different wave-current conditions (a) $U_{cw} = 0.87$, (b) $U_{cw} = 0.16$, (c) $U_{cw} = 0.44$, (d) $U_{cw} = 0.86$. From the figure maximum wave steepness can be seen from fig. 4(c) whereas the lowest wave steepness is observed from fig. 4(d). Fig. 5 shows the plan view of the computational domain used for the analysis of the hydrodynamics around the circular pier. The pile is located in the middle of the wave tank. In the NWT the combined wave-current acting co-directionally. The velocity profiles and the wave elevations are taken by the wave gauges illustrated in fig. 5. The wave gauges are positioned at different locations around the pile. The measurements are taken at 1D from the center of the pile. Fig. 6 shows the numerical results of the free surface elevation for pile for different wave-current conditions. For all the cases maximum free surface wave elevation can be seen at the front of the pile P2. This happens because the wavefront directly strikes the front cylinder. The lowest free surface wave elevation can be seen at the rear side of the pile P3. The free surface elevation is the largest for fig. 6 (c). Due to the increase of wave steepness the free surface wave elevation is highest. Fig. 7. shows the combined inline wave-current forces for different wave-current conditions. Maximum wave forces can be seen for the wave steepness(ak) of 0.229, whereas lowest wave forces are observed for the wave steepness(ak) of 0.024. This happens due to the increase of wave height.

REFERENCES

- Umeyama, M. (2005): Reynolds stresses and velocity distributions in a wave-current coexisting environment. *Journal of waterway, port, coastal, and ocean engineering*, American Society of Civil Engineers, 131(5), 203-212.
- Zhang, Y., Jeng, D.S., Gao, F.P., and Zhang, J.S. (2013). An analytical solution for response of a porous seabed to combined wave and current loading. *Ocean Engineering*, Elsevier, 57, 240-247.
- Wang, J., Geng, L., Ding, L., Zhu, H., and Yurchenko, D. (2020). The state-of-the-art review on energy harvesting from flow-induced vibrations. *Applied Energy*, Elsevier, 267, 114902.
- Bihs, H., Kamath, A., Chella, M. A., Aggarwal, A., & Arntsen, Ø. A. (2016). A new level set numerical wave tank with improved density interpolation for complex wave hydrodynamics. *Computers & Fluids*, 140, 191-208.
- Dutta, D., Bihs, H., & Afzal, M. S. (2022). Computational Fluid Dynamics modelling of hydrodynamic characteristics of oscillatory flow past a square cylinder using the level set method. *Ocean Engineering*, 253, 111211.